TEM Journal. Volume 13, Issue 2, pages 866-874, ISSN 2217-8309, DOI: 10.18421/TEM132-03, May 2024.

Enhancing Savonius Rotor Performance With Zigzag Surface Investigated at Drag Force, Pressure, and Flow Visualization Analysis

Ruzita Sumiati [1,2], Uyung Gatot S. Dinata [1], Dendi Adi Saputra [1]

[1] *Department of Mechanical Engineering, Universitas Andalas, Limau Manis Padang, Indonesia*
[2] *Department of Mechanical Engineering, Politeknik Negeri Padang, Limau Manis Padang, Indonesia*

Abstract **– Savonius, a type of vertical-axis wind turbine, is a small-scale energy conversion device suitable for low wind speeds, such as those characteristic of Indonesian wind speeds, yet has low efficiency. Savonius is a drag-type turbine. Drag force on the surface is affected by roughness or wavyness. The purpose of this study is to analyze the impact of applying wavy (zigzag) variations to the concave surface of Savonius blades on their performance. This was achieved by the use of 3D computational fluid dynamics simulation at TSR 0.6 with a velocity inlet of 5 m/s. The model was semicircular, zigzag on the concave surface on semicircular with t = 0.75, t = 0.25, and t = 1 mm. The result of this study's C_D maximum is 1,817 at the zigzag model with t = 1 and C_D avrg =1.24. The average drag coefficient increased by 14 percent compared to the conventional semicircular rotor. The maximum Cp value is also found at t = 1 mm, which is 0.315. The power coefficient increased by 29 percent compared to the conventional semicircular rotor. The total pressure on the blade shows the highest model with t = 1 mm at the same angle of attack (α = 30). Zigzag on the concave surface affects blade pressure, which improves the performance of the Savonius rotor.**

Keywords **– Savonius rotor, 3D simulations, renewable energy, blade profile, wavy rotor.**

DOI: 10.18421/TEM132-03
https://doi.org/10.18421/TEM132-03

Corresponding author: Uyung Gatot S. Dinata,
Department of Mechanical Engineering, Universitas Andalas, Limau Manis Padang, Indonesia
Email: uyunggsdinata@eng.unand.ac.id

Received: 29 October 2023.
Revised: 07 February 2024.
Accepted: 22 February 2024.
Published: 28 May 2024.

1. Introduction

Extensive use of fossil fuels has resulted in rising carbon dioxide (CO_2) emissions as humanity's reliance on fossil fuels continually grows [1]. The impact of this phenomenon on the area of public health is expected to be substantial. Therefore, advanced nations switch to clean, renewable energy sources (wind and solar energy) in contrast to the increased emissions in developing countries that continue to use coal, especially in Asia [2]. The initial investment for renewable energy provision is quite expensive, hence the need for consideration in choosing the type of renewable energy, such as inexpensive, suitable for small-scale, simple structure, and easy maintenance. The Savonius rotor is a wind-powered green energy device with those advantages. Nevertheless, its efficiency is quite poor. Savonius's limited efficiency can be improved by doing geometric optimization on its aerodynamic properties.

In order to maximize the Savonius rotor's efficiency experts have suggested numerous modifications and refinements to the design. They had examined the effects of diverse design characteristics, such as modification of blade shape [3], [4], [5], [6], variation of overlap ratio [7], [8], [9], endplates [10], [11], aspect ratio [12], number of stage rotors [12], and number of blades [9]. The primary focus of these studies revolves around the examination of the impact of various parameters on its performance. According to a study conducted by Tania *et al.* [13], the Savonius rotor is most efficient while operating at wind speeds below four meters per second, provided that the overlap ratio (OR) is set at 0.15. However, wind speeds over 4 m/s or turbulent wind conditions need an overlap ratio of 0.3. Setiawan *et al.* [14] reported that the performance of Savonius had a significant enhancement of around 62.83% when the overlap ratio was set at 0.2. The recommended overlap of 0.2 has shown greater performance characteristics [9].

The number of blades also influences Savonius performance by increasing the number of blades, which increases their convex area facing the wind at an angle. Thus, increasing the convex area reduces the torque differential between the concave and convex sides and affects Cp [15]. The two-bladed Savonius turbine demonstrated the highest power coefficient in comparison to the 3, 4, 5, and 6 blade configurations [15].

The Savonius rotor uses the disparity in drag between the two blades to his advantage and generates torque [16], [17], [18]. To achieve optimum efficacy, the drag force on the concave blade surface must be greater than that on the convex blade [18]. The impact of wavy or surface roughness is substantial, causing effects on surface drag, heat transfer, and momentum transfer [19]. According to previous studies, the application of waviness to the concave surface has been shown to result in an enhancement in Savonius efficiency [20], [21]. There had not been research conducted about the drag of Savonius rotor with a wavy surface on the concave. The drag value has been shown to have an impact on the efficiency of the helical Savonius turbine [22]. The Savonius rotor's performance is often measured by torque and power coefficient. The investigation of the flow field surrounding the rotor is essential for elucidating the mechanism of power generation in the Savonius rotor [23]. In previous studies, the majority of investigations focused on the conventional semicircular rotor.

The purpose of this investigation is to examine the drag force, pressure, and flow visualization of the Savonius rotor, specifically focusing on the zigzag pattern in the middle of concave surface of the Savonius with variety of zigzag height.

2. Methodology

In this study, the conventional semicircular rotor and a semicircular rotor with a variety of zigzag heights on the concave surface (Fig. 1) were investigated using numerical methods. The models were designed using ZW3D CAD software. The dimensions of all models are identical, with the only distinction being the zigzag height at the concave surface. Table 1 presents the geometric parameters of the Savonius rotor.

Table 1. Geometric parameter of model purpose

Parameter	Value
Blade Diameter	200 mm
Endplate	220 mm
Overlab ratio	0.2
Wind speed	5 m/s
Height of blade	200 mm
Number of blade	2
Number of stage	1
Aspect Ratio	1
TSR	0.6
Variety of Zigzag height (t)	0.25 mm, 0.75 mm & 1 mm

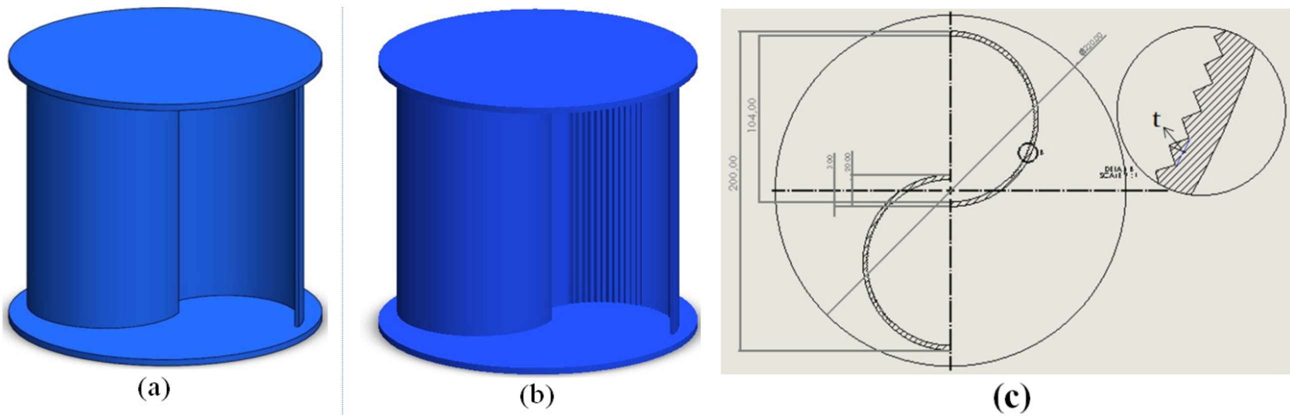

Figure 1. Sketch and geometric parameters (a) Conventional semicircular rotor (b) Conventional with zigzag pattern on the concave surface rotor (c) geometry detail of zigzag pattern

2.1. Numerical Method

This study employed the Computational Fluid Dynamics ANSYS 2020 R2. Using unstructured triangular grids, the 3D computational domains have been discretized. Fig. 2 depicts the computational domain, which has dimensions of 30R x 10R x 10R.

The domain is separated into two distinct regions: a stationary and a rotating section. The two components are separated by an interface. Fine grids are often used for spinning components, with the inclusion of up to 20 layers and 1.2 growth ratio rate. Blade inflations are included in order to get precise data from the test item, namely the blades.

In general, inflation layers are also a component of meshing and are utilized when it is necessary to capture the turbulent flow that is wall-bounded in the boundary layer. The mesh of rotating sub domain and surface of blade are shown in Fig. 3.

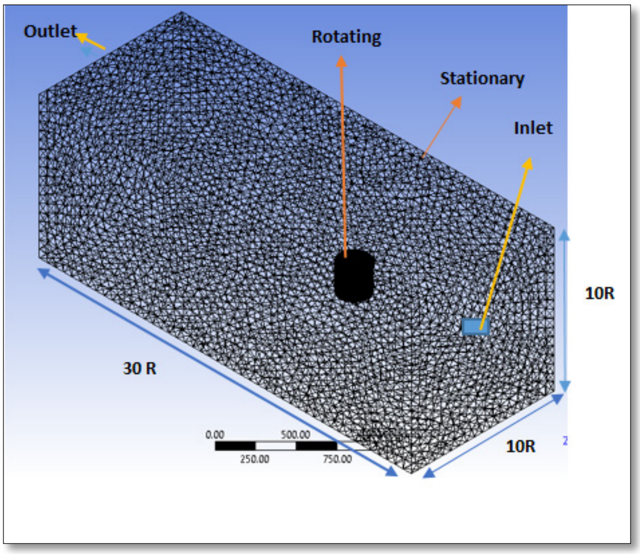

Figure 2. Computational domain

The commercial CFD program Ansys Fluent academic version was used to simulate the flow field around the blade, employing the Unsteady Reynolds-Averaged Navier-Stokes (URANS) equations. Additionally, the k-ω shear stress transfer (SST) model was used to represent the turbulent viscosity. Cell zone condition set a mesh motion at rotating sub domain with TSR 0.6. The boundary conditions contain: inlet with constant velocity of 5 m/s, pressure outlet of 0 Pa, the interfaces are designated as the overlapping edges between the rotating and the stationary domain and the blades are subject to no-slip wall conditions at their surfaces.

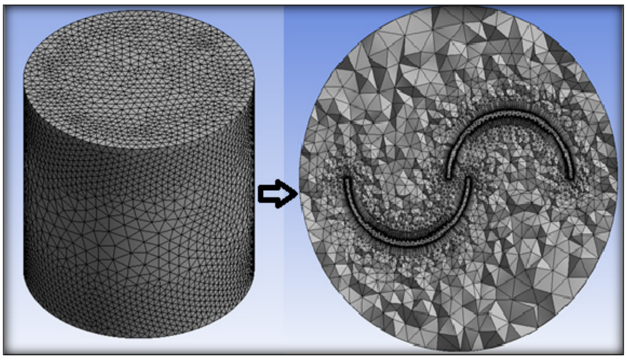

Figure 3. Mesh for rotating sub domain and around the blade

The sliding mesh technique can be employed to dynamically simulate the rotation of a turbine for the generation of electricity from the input stream.

The number of iterations required for convergence thresholds to be met or reached can be computed at each site. The convergence threshold refers to the upper limit of the proportion of pixels that will retain their cluster allocations between rounds. The time step size has been equated to the angle of increase (θ) for every rotation step. The calculation was performed for every rotating position. Equations 1 and 2 present the formula used to sum up the time steps and time step size.

$$\text{Time step size (TSS)} = \frac{\text{N}}{\text{Sum of time steps} \ \text{x} \ 0{:}15915 \ \text{x} \ \omega} \quad (1)$$

$$\text{Sum of time steps} = \text{N}\frac{360}{\theta} \quad (2)$$

The symbol of the rotation number is N, the spin direction is θ , and the rotational speed is ω. The ω data from the TSR values are shown in Table 2. These will be used to calculate how efficient the Savonius turbine is.

Table 2. Data rotation speed base on different TSR

λ	U (m/s)	R (m)	ω (rad/s)	N (rpm)	TSS (s)
0.5	5	0.1	25	238.85	0.000875
0.6	5	0.1	30	286.6	0.000581
0.7	5	0.1	35	334.4	0.000498
0.8	5	0.1	40	382.2	0.000436

Applying a SIMPLE scheme for pressure-velocity coupling improves stability. Table 3 presents the summery of solution methods.

Table 3. The summery of solution methods

Pressure/velocity coupling	SIMPLE
Spatial discretization	
• Gradient	Least squares cell based
• Pressure	Second order upwind
• momentum	Second order upwind
Transiente Formulation	Second order implicit

2.2. Calculating Savonius Performance

Coefficient of torque (C_T) and coefficient of power (Cp) are the two main parameters that affect the Savonious' performance [24]. Cp measures the turbine's performance in generating kinetic energy into mechanical energy [25], which is calculated using Eq. 3, the ratio between the actual power of the turbine (P) and the available power in the wind (P_A). The C_T value compares the actual torque produced with the torque available in the wind, as expressed by Eq. 4. TSR (λ) is the ratio between the speed of the rotor tip and the wind speed expressed by Eq. 5.

$$C_p = \frac{P}{P_A} = \frac{T.\omega}{\frac{1}{2}\rho\, A\, U^3} \quad (3)$$

$$C_T = \frac{T}{T_A} = \frac{T}{\frac{1}{2}\rho\, A\, U^2 R} \quad (4)$$

$$TSR\ (\lambda) = \frac{\omega\, R}{U} \quad (5)$$

Where ρ is the density of air measured in kg/m^3, U is the speed of the wind in the free stream measured in m/s, A is the swept area of the turbine measured in square meters (m^2), equal to the height multiplied by the rotor diameter (m^2), R is the radius of the turbine measured in meters, and ω is the rotational speed of the turbine measured in rad/s.

2.3. Validation Data

The computational simulation technique begins with a verification process of the parameters of the present simulation analysis with previous work before beginning on the simulation illustrated in Fig. 4. Unsteady simulations are performed with the SST k-ω turbulence model at TSR 0.6. and U = 6.2 m/s

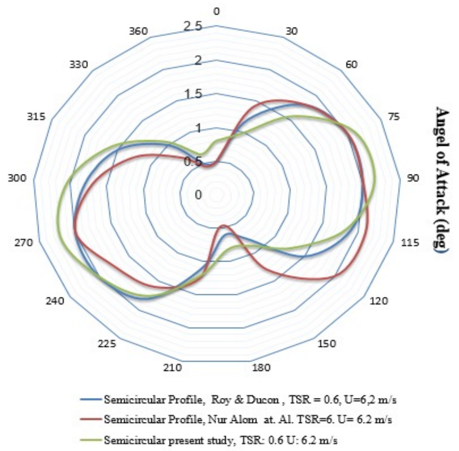

Figure 4. Validation of the coefficient drag using the previously collected data

The current analysis exhibits a similar graphical pattern in C_D value to the two prior investigations conducted by Nur Alom [22], Roy and Ducoin [26]. Their studies used a 2D numerical simulation method, whereas this research adopts a 3D simulation. Consequently, there is a slight discrepancy in the coefficient drag results. The current investigation exhibits a slightly higher drag coefficient (C_D) when compared to the two preceding models. Although the C_D value is not exactly the same, it has approached the pattern of data values in previous studies.

3. Results and Discussion

In this section, the numerical results obtained are presented in the form of turbine performance (C_P & C_T), drag coefficient, pressure couture, and flow visualization.

3.1. Performance Analysis of C_P and C_T

C_P and C_T values are calculated at TSR 0.5 - 0.8 and U = 5 m/s, using semicircular and zigzag models in the middle of concave surfaces with t = 1mm and t= 0.75 mm. Fig. 5 illustrates a comparison of the coefficient of performance (C_P) among conventional semicircular turbine, turbine with zigzag (t= 0.75mm) and, turbine with zigzag (t=1 mm) in accordance with the results obtained from numerical simulations. The computation of C_P, is performed by using the peak torque obtained from a single revolution of the turbine.

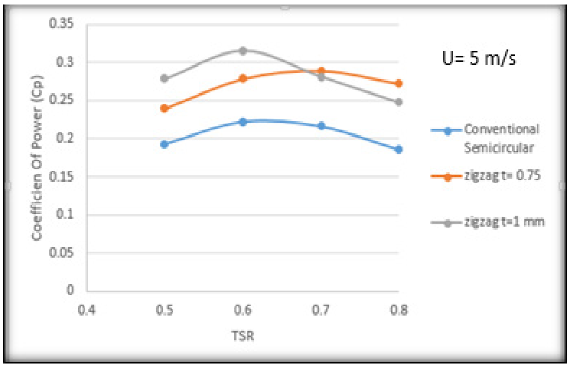

Figure 5. Coefficient of power

Figure 6 presents the torque coefficient graph for the TSR variation. The graph indicates that the Savonius rotor with zigzag configuration exhibits a better Cp, achieving the highest Cp value of 0.315 at zigzag t = 1 and TSR 0.6. This Cp value represents a 29 percent increase compared to the semicircular configuration.

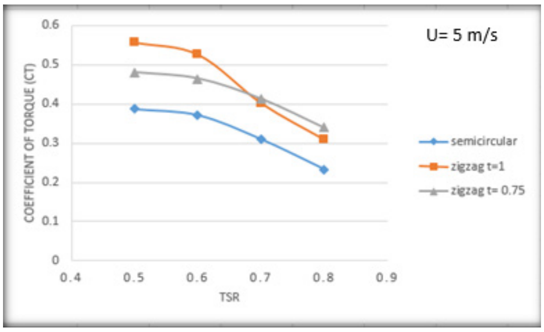

Figure 6. Coefficient of torque

The relationships between C_T and TSR for the purpose model shown in Fig. 6 depict C_T increasing as the TSR falls. This graph trend appears to be consistent with previous studies [27], [10]. Both of the Savonius models with zigzag on the concave surface have a higher coefficient than the conventional Savonius. The presence of zigzags in the middle of the concave surface of the Savonius rotor has been shown to have a beneficial impact on its efficiency.

The increase in efficiency may be ascribed to the elevated drag encountered on the concave side with the zigzag pattern. The geometric configuration of this design enhances the difference in force between the concave and convex blades, resulting in a significant increase in the amount of torque. The subsequent increase in torque has a noticeable impact on the overall performance of the Savonius rotor. In sub-topic 3.2, a comparison of the drag coefficients of the studied models will be shown.

3.2. Drag Coefficient

Preliminary 3D simulations were conducted in order to assess the impact of varying zigzag sizes on the concave surface on drag coefficients. The drag coefficients for zigzag in the middle of concave surface and conventional semicircular with different angle of attack are shown in Fig. 7.

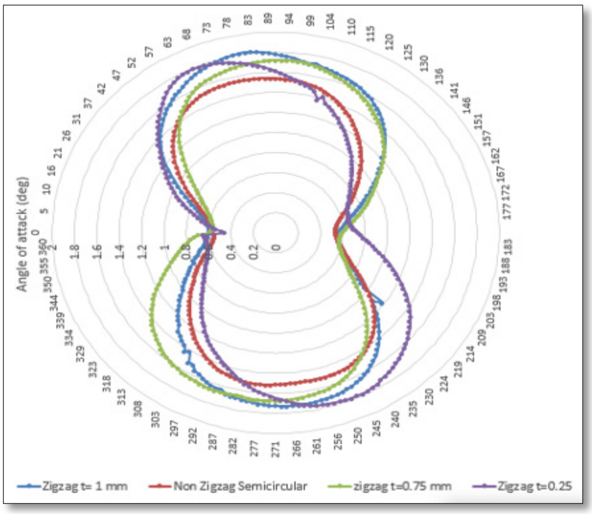

Figure 7. C_D of model at TSR 6 & U=5 m/s

Compared to conventional semicircular rotor, the zigzag model achieves a higher C_D. In Figure 7, the $C_{D\ max}$ values for the zigzag model with t = 0.75 are observed at α = 96° and 275°, for the zigzag model with t = 1 at α = 82° and 266°, and for the zigzag model with t=0.25 at α = 68° and 249°. Meanwhile, the $C_{D\ max}$ for the conventional semicircular model occurs at α = 82° and 277°. Models with zigzag height variations, namely t = 0.25, t = 0.75, and t = 1, show that the highest drag coefficient is found at t = 1, which is 1.8178. For the semicircular drag coefficient, it is 1.546. Based on the investigation of the four models, it is evident that the Savonius rotor model with a zigzag configuration on the concave surface exhibits a higher drag coefficient compared to the conventional semicircular model.

Nur Alom's research [22] on drag force suggests that an increase in drag value has a beneficial effect on the efficiency of the Savonius rotor.

This discovery substantiates earlier scholarly findings [20], [21], which suggest that augmenting the surface roughness on the concave side of the Savonius turbine results in a heightened level of efficiency.

The average drag coefficients generated by the four turbine models can be seen in Fig. 8.

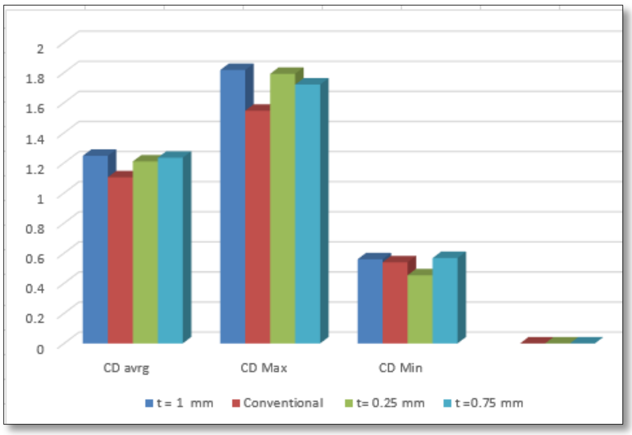

Figure 8. Comparison C_D max, C_D Avrg & C_D min

Fig. 8 shows that of the four models analyzed numerically, the average drag coefficient value shows that the application of zigzag on the concave surface has a better average drag coefficient value than the semicircular one. The research by Khairil Anwar [28] on Savonius rotors said that adding a variable straight blade angle to the Savonius configuration raises the drag coefficient, which makes the Savonius turbine more efficient. Consequently, the heightened drag force significantly impacts the overall efficiency of the Savonius rotor.

There is evidence that an increase in the average drag value affects the increase in turbine efficiency. This was found by calculating turbine efficiency (Cp and Ct) and analyzing drag coefficients. However, the maximum size limit of zigzag that positively affects the efficiency value is not yet known. Further research is still needed because a large zigzag will affect turbulence and noise, which will impact rotor performance.

3.3. Pressure Contour

The contour plots provide forecasts of the variations in velocity and pressure in various regions surrounding blades throughout the flow domain. The pressure contours illustrate the presence of a reduction in pressure over the rotor, spanning from the upstream region to the downstream region. The visible pressure decrease is due to the mechanical effort exerted by the rotor in order to generate rotational motion.

Fig. 9(a-d) presents the four models that have been studied. The models were observed at an angle of attack of 30° and an inlet velocity of 5 m/s. According to the pressure contours observed in the all models, the highest total pressure is found in the 1 mm zigzag. Model with t = 1 mm zigzag has a higher pressure than the others.

Based on the simulation results depicting pressure contours for the four models, a noticeable distinction becomes evident. In the case of the semicircular model, there is an almost uniform pressure distribution on both the concave and convex sides, resulting in a relatively modest torque effect. Conversely, when we examine the zigzag model, it is apparent that the pressure on the concave side exceeds that on the convex side. This variance in pressure distribution diminishes the adverse force, consequently yielding a more substantial torque in comparison to the semicircular model.

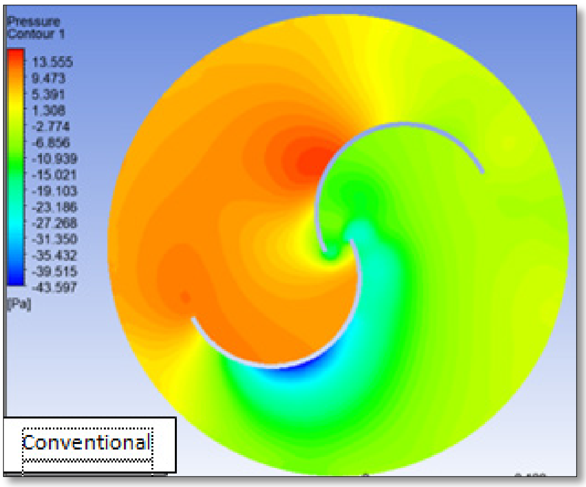

Figure 9(a). Pressure contour conventional rotor

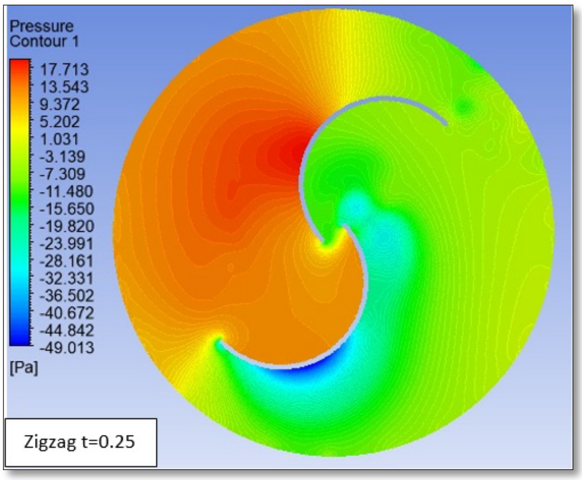

Figure 9(b). Pressure contour of the zigzag t= 0.25mm

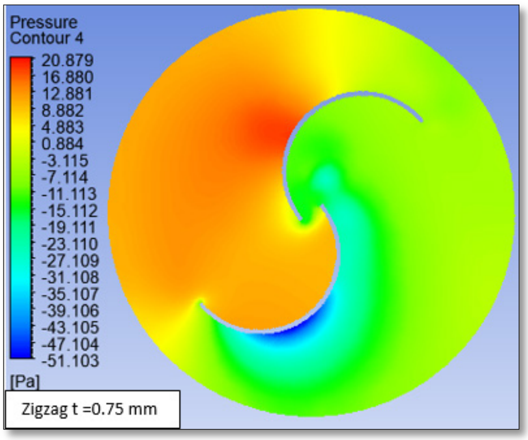

Figure 9(c). Pressure contour of the zigzag t=0.75mm

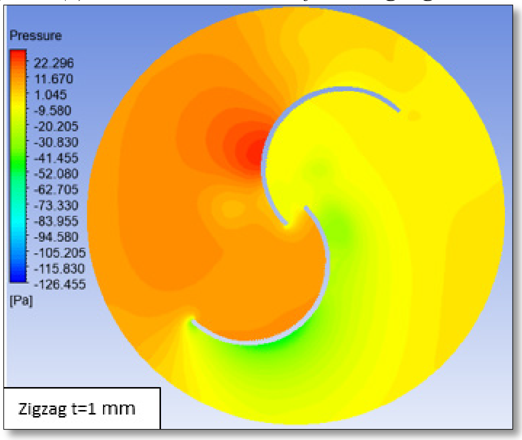

Figure 9(d). Pressure contour of zigzag t =1mm

3.4. Velocity Contours

The velocity contours of the Savonius turbine profile were analyzed at an inlet velocity of 5 m/s. The velocity energy contacting the concave wall is converted into kinetic energy, which reduces the speed at the concave.

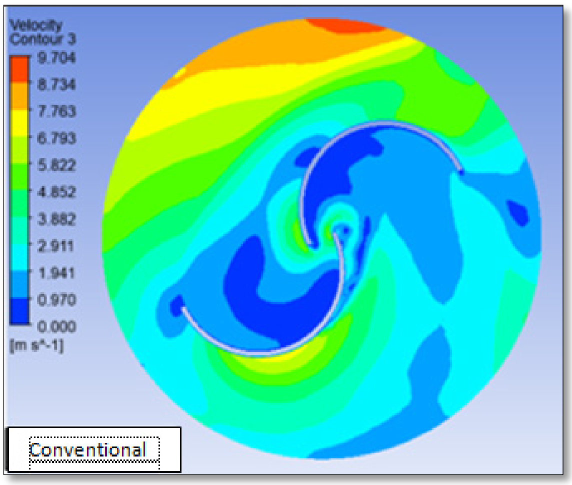

Figure 10(a). Velocity contour of convensional rotor

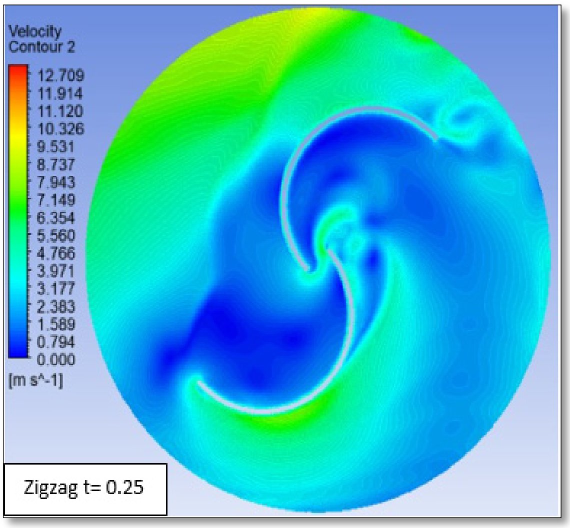

Figure 10(b). Velocity contour of the zigzag t=0.25 mm

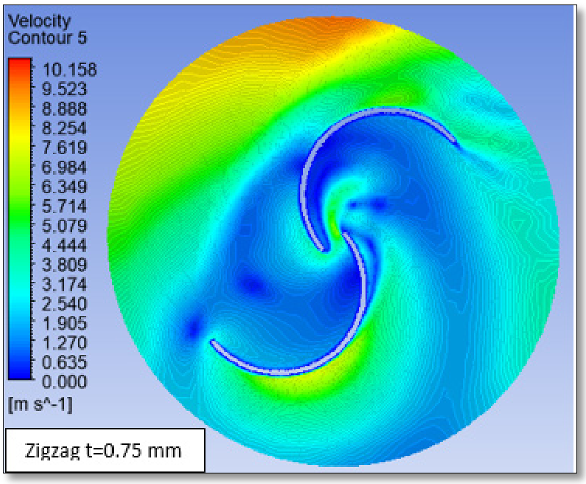

Figure 10(c). Velocity contour of the zigzag t= 0.75 mm

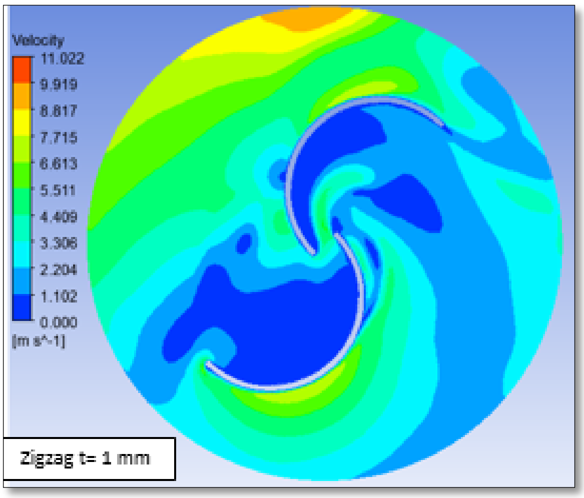

Figure 10(d). Velocity contour of the zigzag t=1mm zigzag

In Figure 10(a-d), the blue color (velocity = 0 m/s) at the area concave surface makes it evident that the Savonius turbine with a zigzag configuration exhibits a region of reduced wind speed on its concave side. This phenomenon can explain the conversion of the kinetic energy of the fluid into pressure energy.

An area with a velocity of 0 m/s on a concave surface indicates that the zigzag surface model has a larger area compared to the conventional Savonius. Additionally, the zigzag model demonstrates a more pronounced transfer of wind power to the returning blade side within the overlap area, which has the potential to enhance the efficiency of the Savonius turbine.

In the zigzag model, particularly at t=1 mm, a disparity in velocity emerges between the convex and concave sections of the advancing blade, with greater velocities observed on the convex sides. This velocity difference results in a positive torque being exerted on the advancing blade. These observations furnish compelling evidence in favor of the hypothesis that the pressure differential within the zigzag (wavy) rotor exceeds that of the conventional rotor.

4. Conclusion

This study was a numerical method for investigating the drag coefficient and pressure couture characteristic with variety of surface roughness with zigzag pattern on the middle of concave surface. The data illustrates that the drag and pressure values increase with increasing size of zigzag values. The addition of zigzag pattern in the concave will increase drag force which can be influential in increasing the power of the Savonius turbine.

This conducted research has limitations: it solely focuses on discussing 3D simulation with a single model for inlet velocity of 5 m/s at TSR 6, utilizing the incompressible, URANS equations and the k-ω shear stress transfer (SST) turbulent viscosity model. Furthermore, it has not been implemented in experimental tests

Acknowledgements

This work was supported by Doctoral Dissertation Research Grant, from Ministry of Education and Culture Republic of Indonesia (Grant No. 131/UN16.19/PT.01.03/2023). Furthermore, the authors also gratefully acknowledged for the facilities support provided by Universitas Andalas, West Sumatera, Indonesia during the research.

References:

[1]. Liu, Z., Deng, Z., Davis, S. J., Giron, C. & Ciais, P. (2022). Monitoring Global Carbon Emissions in 2021. *Nat Rev Earth Environ 3,* 217–219. Doi: 10.1038/s43017-022-00285-w

[2]. O'Neill, S. (2020). Global CO2 Emissions Level Off in 2019, with a Drop Predicted in 2020. *Engineering 6,* 958–959. Doi: 10.1016/j.eng.2020.07.005.

[3]. Tartuferi, M., D'Alessandro, V., Montelpare, S. & Ricci, R. (2015). Enhancement of Savonius Wind Rotor Aerodynamic Performance: A Computational Study Of New Blade Shapes And Curtain Systems. *Energy 79*, 371–384. Doi: 10.1016/j.energy.2014.11.023.

[4]. Mohan, M. & Saha, U. K. (2023). Computational Study of A Newly Developed Parabolic Blade Profile of a Savonius Wind Rotor. *J Braz. Soc. Mech. Sci. Eng. 45*, 548. Doi: 10.1007/s40430-023-04474-6.

[5]. Rizk, M. & Nasr, K. (2023). Computational Fluid Dynamics Investigations Over Conventional and Modified Savonius Wind Turbines. *Heliyon 9*, e16876. Doi: 10.1016/j.heliyon.2023.e16876.

[6]. Tian, W., Mao, Z., Zhang, B. & Li, Y. (2018). Shape Optimization of A Savonius Wind Rotor With Different Convex And Concave Sides. *Renewable Energy 117*, 287–299. Doi: 10.1016/j.renene.2017.10.067.

[7]. Dewan, A., Bishnoi, A. K., Singh, T. P. & Tomar, S. S. (2023). Elliptical Bladed Savonius Rotor for Wind Energy: Efficacy of RANS Modeling for Flow Characteristics. *Journal of Energy Resources Technology 145*, 051301. Doi: 10.1115/1.4056275.

[8]. Hassanzadeh, R. & Mohammadnejad, M. (2019). Effects of Inward And Outward Overlap Ratios On The Two-Blade Savonius Type of Vertical Axis Wind Turbine Performance. *International Journal of Green Energy 16*, 1485–1496. Doi: 10.1080/15435075.2019.1671420.

[9]. Thiyagaraj, J., Rahamathullah, I., Anbuchezhiyan, G., Barathiraja, R. & Ponshanmugakumar, A. (2021). Influence of Blade Numbers, Overlap Ratio And Modified Blades On Performance Characteristics Of The Savonius Hydro-Kinetic Turbine. *Materials Today: Proceedings 46*, 4047–4053. Doi: 10.1016/j.matpr.2021.02.568.

[10]. Al-quraishi, B. A. J., Kadhum Aboaltabooq, M. H. & K. AL-Fatlwe, F. M. (2022). A Simulation Investigation The Performance Of A Small Scale Elliptical Savonius Wind Turbine With Twisting Blades And Sloping Ends Plates. *PEN, 10*, 376. Doi: 10.21533/pen.v10i1.2392.

[11]. Micha Premkumar, T., Sivamani, S., Kirthees, E., Hariram, V. & Mohan, T. (2018). Data Set on The Experimental Investigations of A Helical Savonius Style Vawt With And Without End Plates. *Data in Brief, 19*, 1925–1932. Doi: 10.1016/j.dib.2018.06.113.

[12]. Saad, A. S., Ookawara, S. & Ahmed, M. (2022). Influence of Varying the Stage Aspect Ratio on the Performance of Multi-Stage Savonius Wind Rotors. *Journal of Energy Resources Technology 144*, 011301. Doi: 10.1115/1.4050876.

[13]. Tania, R. at. al. (2018). Experimental Investigation on the Influence of Overlap Ratio on Savonius Turbines Performance. *IJRER, 8*(3). Doi:10.20508/ijrer.v8i3.7764.g7480.

[14]. Setiawan, P. A., Indarti, R., Ariwiyono, N., Yuwono, T. & Widodo, W. A. (2021). An Experimental Study of Overlap Ratio Effect to Savonius Water Current Turbine by Using Myring Equation for n=1. *J. Phys.: Conf. Series., 1764*(1), 012198. Doi: 10.1088/1742-6596/1764/1/012198.

[15]. Al-Kayiem, H. H., Bhayo, B. A. & Assadi, M. (2016). Comparative Critique on The Design Parameters And Their Effect on The Performance of S-Rotors. *Renewable Energy, 99*, 1306–1317. Doi: 10.1016/j.renene.2016.07.015

[16]. Fatahian, E., Ismail, F., Hafifi Hafiz Ishak, M. & Shyang Chang, W. (2022). An innovative Deflector System for Drag-Type Savonius Turbine Using a Rotating Cylinder for Performance Improvement. *Energy Conversion and Management, 257*, 115453. Doi: 10.1016/j.enconman.2022.115453 .

[17]. Dewan, A., Gautam, A. & Goyal, R. (2021). Savonius Wind Turbines: A Review of Recent Advances in Design and Performance Enhancements. *Materials Today: Proceedings, 47*, 2976–2983. Doi: 10.1016/j.matpr.2021.05.205.

[18]. Yuwono, T., Sakti, G., Nur Aulia, F. & Chandra Wijaya, A. (2020). Improving The Performance of Savonius Wind Turbine By Installation Of A Circular Cylinder Upstream of Returning Turbine Blade. *Alexandria Engineering Journal, 59*(6), 4923–4932. Doi: 10.1016/j.aej.2020.09.009.

[19]. Gao, W., Samtaney, R. & Parsani, M. (2022). Direct Numerical Simulation Of Transitional Flow Past An Airfoil with Partially Covered Wavy Roughness Elements. *Physics of Fluids, 34*(10), 105135. Doi: 10.1063/5.0123437.

[20]. Mohanad Al-Ghriybah & Djamal Hissein Didane. (2023). Performance Improvement of a Savonius Wind Turbine Using Wavy Concave Blades. *CFDL 15*(9), 32–44. Doi: 10.37934/cfdl.15.9.3244

[21]. Nurmutia, S., Manshoor, B., Khalid, A., Zaman, I., Didane, D. H., Haq, R. H. A., ... & Ibrahim, M. N. (2023). Performance Analysis on a New Design of Blade Shape for Savonius Wind Turbine. *Journal of Advanced Research in Fluid Mechanics and Thermal Sciences*, *108*(1), 173-183.

[22]. Alom, N., Borah, B., & Saha, U. K. (2018). An insight into the drag and lift characteristics of modified Bach and Benesh profiles of Savonius rotor. *Energy Procedia*, *144*, 50-56.

[23]. Fujisawa, N. & Gotoh, F. (1992). Pressure Measurements And Flow Visualization Study Of A Savonius Rotor. *Journal of Wind Engineering and Industrial Aerodynamics, 39*, 51–60, Doi: 10.1016/0167-6105(92)90532-F.

[24]. Sonawane, C. R., Sasar, Y., Shaikh, M., Kokande, Y., Mustafa, M., & Pandey, A. (2022). Numerical simulation of Savonius rotors used for low wind speed application. *Materials Today: Proceedings*, *49*, 1610-1616.

[25]. Al Absi, S. M., Jabbar, A. H., Mezan, S. O., Al-Rawi, B. A., & Al_Attabi, S. T. (2021). An experimental test of the performance enhancement of a Savonius turbine by modifying the inner surface of a blade. *Materials Today: Proceedings*, *42*, 2233-2240.

[26]. Roy, S., & Ducoin, A. (2016). Unsteady analysis on the instantaneous forces and moment arms acting on a novel Savonius-style wind turbine. *Energy Conversion and Management*, *121*, 281-296.

[27]. Tjahjana, D. D. D. P. et al. (2021). Experimental Study of The Effect of Slotted Blades on The Savonius Wind Turbine Performance. *Theoretical and Applied Mechanics Letters, 11,* 100249.

[28]. Anwar, K., Himran, S., Sule, L. & Azis, N. (2018). Numerical L Investigation Of Modified Savonius Wind Turbine With Various Straight Blade Angle. *Journal of Mechanical Engineering Research & Developments, 41*, 38–42.